Lessons of Many-Body Quantum Mechanics for Circuit Design

Kun Zhang, Kwangmin Yu, Kun Hao, Vivek Kumar Singh,
Pramod Padmanabhan, Vladimir Korepin

Sept 30, 2024

Center for Quantum and Topological Systems, NYU Abu Dhabi

Outline

- Two distinguished classes of models in many-body QM. In free models the dynamics is 1-body reducible. In BA solvable the dynamics is 2-body reducible.
- General theories about the two-qubit gate
  - Gate-based decomposition
  - Pulse-based decomposition
- Braid gate and Yang-Baxter gate (YBG)
  - All families of braid gates
  - YBGs from the Yang-Baxterization
- Realization of YBGs on quantum computers
- Conclusions and outlooks

Background

The Yang-Baxter gate is the key element connecting the study of quantum computation and integrable system.

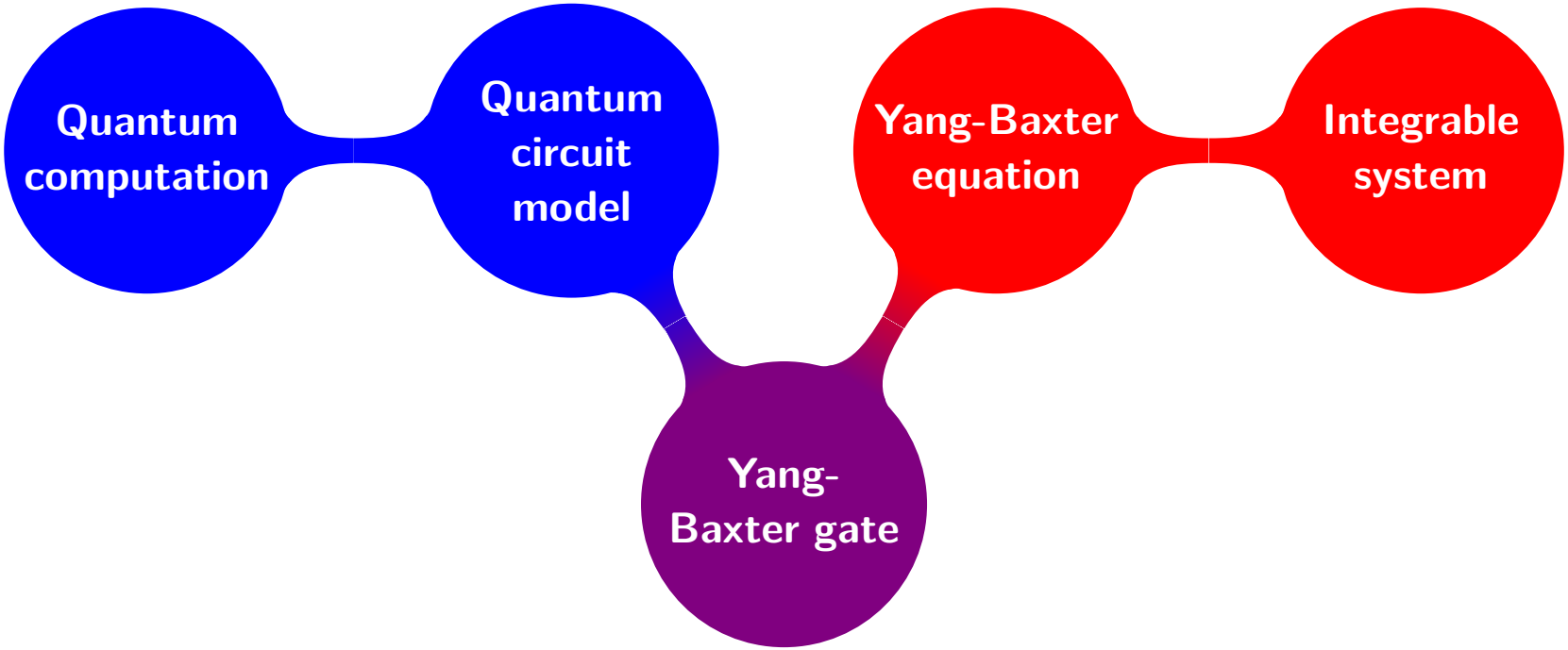

Yang-Baxter equation

- The Yang-Baxter equation (YBE) plays the central role in the study of integrable models.

$$\check{R}_{12}(\mu_1)\check{R}_{23}(\mu_1+\mu_2)\check{R}_{12}(\mu_2) = \check{R}_{23}(\mu_2)\check{R}_{12}(\mu_1+\mu_2)\check{R}_{23}(\mu_1).$$

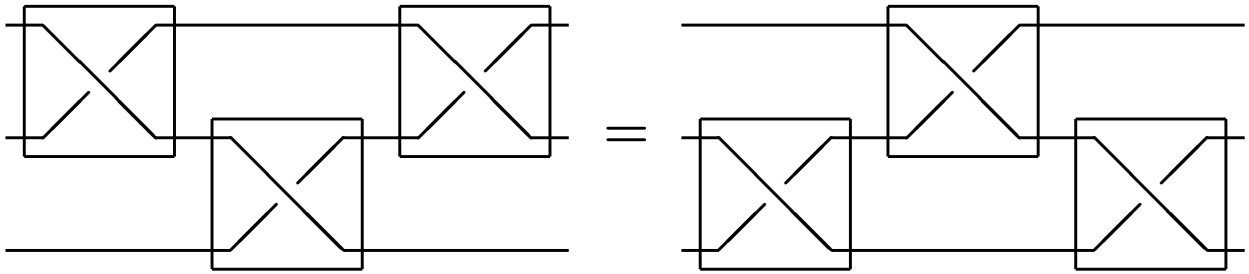

- The Yang-Baxter equation reduces to the braid group relation, given by

$$\check{B}_{12}\check{B}_{23}\check{B}_{12} = \check{B}_{23}\check{B}_{12}\check{B}_{23}.$$

Why Yang-Baxter gate?

- The braid gate is introduced because of the topological quantum computing (A. Kitaev, M. H. Freedman, Z.-H. Wang).
- The braid gate is introduced to study the relationship between the topological entanglement and quantum entanglement (S. J. Lomonaco Jr., L. H. Kauffman).
- Quantum simulation of integrable spin chain via the Suzuki-Trotter decomposition is realized by YBG. The simulation circuit is integrable (T. Prosen, I. L. Aleiner, Y. Miao).
- The algebraic Bethe ansatz can be applied to study the integrability of quantum cellular automaton (B. Pozsgay).
- The properties of many-body nonequilibrium dynamics can be probed from the integrable circuit.

Trotter decomposition

- Consider the XXX model

$$H_{XXX} = \frac{J}{2} \sum_{j=1}^{2N} (1 + \vec{\sigma}_j \cdot \vec{\sigma}_{j+1}),$$

with the Pauli vector $\vec{\sigma}_j$.

- Consider the Trotter product formula

$$e^{-itH} = \lim_{n \to \infty} \left(e^{-\frac{itH_{\text{even}}}{n}} e^{-\frac{itH_{\text{odd}}}{n}} \right)^n.$$

- Then for large n, the evolution of XXX model can be approximated by applying

$$U_{j,j+1} = \exp\left(-\frac{iJt}{2n} (1 + \vec{\sigma}_j \cdot \vec{\sigma}_{j+1}) \right)$$

on even and odd sites interchangeably.

Trotter circuit

Trotter circuit with a nearest-neighbor interaction. The figure is from [M. Vanicat, L. Zadnik, T. Prosen, arXiv:1712.00431].

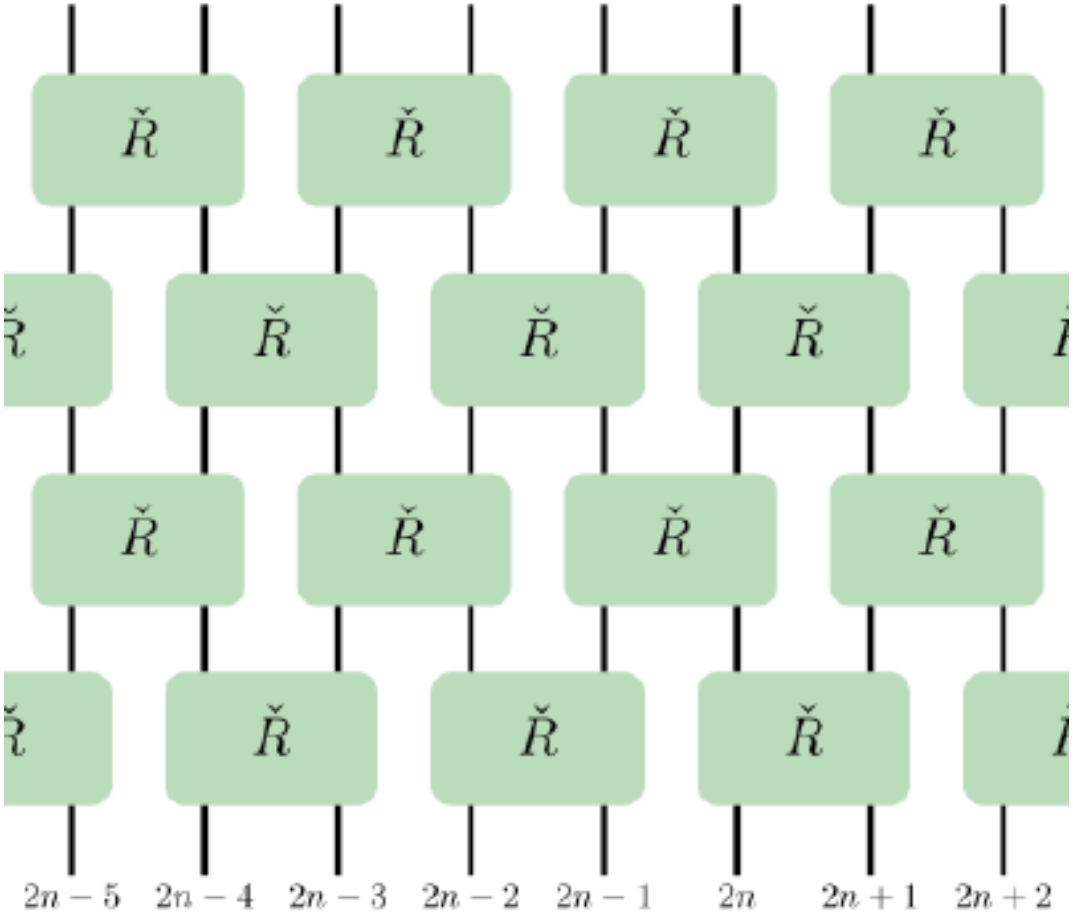

Transfer matrix

- The Trotter circuit has the transfer matrix

$$T(\lambda) = \mathrm{Tr}_0 \left(\overleftarrow{\prod_{1 \le j \le N}} R_{0j}\left(\lambda - (-1)^j \frac{\phi}{2}\right) \right),$$

with $R(\lambda) = P\check{R}(\lambda)$, $\phi = -tJ/n$, and the right to left order of product [M. Vanicat, L. Zadnik, T. Prosen, arXiv:1712.00431].

- The evolution of the whole circuit is given by $\mathcal{U}^n(\phi)$. One layer of evolution is given by

$$\mathcal{U}(\phi) = T\left(-\frac{\phi}{2}\right)^{-1} T\left(\frac{\phi}{2}\right)$$

Conserved charges

- The circuit has the conserved charges

$$Q_n^{\pm} = \frac{d^n}{d\lambda^n} \log T(\lambda)\Big|_{\lambda=\pm\frac{\phi}{2}}.$$

- For $n = 1$, we have

$$Q_1^{+} = \sum_{n=1}^{N/2} q^{[1,+]}_{2n-2,2n-1,2n}, \qquad Q_1^{-} = \sum_{n=1}^{N/2} q^{[1,-]}_{2n-1,2n,2n+1}.$$

with the local charge density

$$q^{[1,\pm]}_{1,2,3} = \frac{i}{2(1+\phi^2)} \left(\vec{\sigma}_1 \cdot \vec{\sigma}_2 + \vec{\sigma}_2 \cdot \vec{\sigma}_3 + \phi^2 \vec{\sigma}_1 \cdot \vec{\sigma}_3 \mp \phi \vec{\sigma}_1 \cdot (\vec{\sigma}_2 \times \vec{\sigma}_3) \right).$$

- At Trotter limit $\phi \to 0$, the charge density returns back to the Hamiltonian density.

Experiments

Integrable circuit can be well characterized. It is practical to firstly realize the integrable circuit on computers. Then consider the integrable-breaking dynamics.

- Google studied the bound state in the XXZ integrable circuit. Then showed that the resilience of the bound states to integrability breaking [A. Morvan et al., arXiv:2206.05254].
- The conserved charges have been measured on quantum computers. Due to noises, the conserved charges decay through time [K. Maruyoshi, et al., arXiv:2208.00576].
- The spin transport of integrable circuits is studied on quantum computers. The results show the Kardar-Parisi-Zhang scaling [N. Keenan, et al., arXiv:2208.12243].

Universal quantum gate

- In classical reversible computation, three-bit gate is required in order to do any computation.
- Remarkbly, two-qubit gates are universal for quantum computation [D. P. Divincenzo, arXiv:cond-mat/9407022].
- Any two-qubit gate, which can generate quantum entanglement, combined with single-qubit gates, is universal, known as Brylinski's theorem [J. L. Brylinski, R. Brylinski, quant-ph/0108062].
- Common two-qubit gates include

$$\text{CNOT} = |0\rangle\langle 0| \otimes \mathbb{1}_2 + |1\rangle\langle 1| \otimes \sigma_x;$$

$$R_{zz}(\theta) = e^{-\frac{i}{2}\theta\sigma_z\otimes\sigma_z}.$$

- Many-qubit gates.
  Tofoli gates satisfy the tetrahedron equations [multi-dimensional generalization of Yang-Baxter] `https://arxiv.org/pdf/2405.16477`

Nonlocal parameters

- Any two-qubit gate $U \in SU(4)$ can be decomposed into [B. Kraus, J. I. Cirac, arXiv:quant-ph/0011050]

$$U = (V_1 \otimes V_2) e^{\frac{i}{2}\left(a_1 \sigma_x \otimes \sigma_x + a_2 \sigma_y \otimes \sigma_y + a_3 \sigma_z \otimes \sigma_z\right)} (V_3 \otimes V_4),$$

  with $V_k \in SU(2)$ $(k = 1, 2, 3, 4)$. Only the parameters $[a_1, a_2, a_3]$, called the nonlocal parameters, determine the entangling properties of U.

- Consider the average entropy generated by U, called the entangling power [P. Zanardi, et al., arXiv:quant-ph/0005031],

$$e_p(U) = \overline{E(U|\psi_1\rangle \otimes |\psi_2\rangle)}_{|\psi_1\rangle \otimes |\psi_2\rangle},$$

  with the linear entropy of two-qubit state $E(|\Psi\rangle) = 1 - \mathrm{Tr}_1 \rho^2$ and $\rho = \mathrm{Tr}_2 |\Psi\rangle\langle\Psi|$.

- The entangling power of two-qubit gate has the analytical form [S. Balakrishnan, R. Sankaranarayanan, arXiv:1005.2467]

$$e_p(U) = \frac{2}{9}(1 - \cos^2 a_1 \cos^2 a_2 \cos^2 a_3 - \sin^2 a_1 \sin^2 a_2 \sin^2 a_3).$$

Geometric representation

The two-qubit gate has the geometric picture given by the Weyl chamber with $A_1 = [\pi, 0, 0]$, $A_2 = [\pi/2, \pi/2, 0]$, and $A_3 = [\pi/2, \pi/2, \pi/2]$, called the two-qubit tetrahedron [J. Zhang, et al., arXiv:quant-ph/0209120].

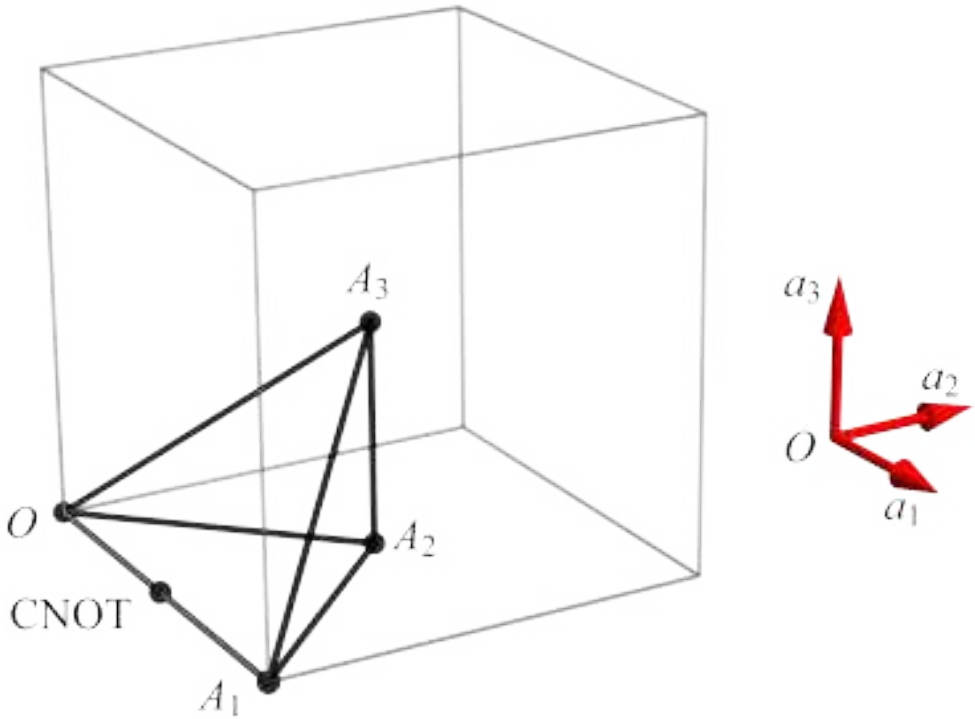

Gate decomposition

- **Theorem 1** *Any two-qubit gate* $[U] = [a_1, a_2, a_3]$ *can be constructed from minimal* n $(n \geq 3)$ *applications of* $R_{zz}(\theta)$ *gate, if the nonlocal parameters satisfies* $0 \leq a_1 + a_2 + a_3 \leq n\theta$ *or* $a_1 - a_2 - a_3 \geq \pi - n\theta$ [J. Zhang, et al., arXiv:quant-ph/0308167].

- **Theorem 2** *A two-qubit gate with the nonlocal parameters* $[U] = [a_1, a_2, a_3]$ *can generate the maximal entangled state from the product state iff*

$$\frac{\pi}{2} \leq a_j + a_k \leq a_j + a_l + \frac{\pi}{2} \leq \pi,$$

or

$$\frac{3\pi}{2} \leq a_j + a_k \leq a_j + a_l + \frac{\pi}{2} \leq 2\pi.$$

Here (j, k, l) *is the permutation of* $(1, 2, 3)$ with $j \neq k \neq l$ [J. Zhang, et al., arXiv:quant-ph/0209120].

Cross-resonance operation

- Cross-resonance (CR) is a technique used in the field of quantum computation to implement controlled operations between qubits in a superconducting qubit architecture.
- It relies on the interaction between two qubits, where one qubit is driven at the frequency corresponding to the resonance frequency of the other qubit.
- In a typical setup involving two qubits, known as the target qubit and control qubit, the control qubit is driven at its resonance frequency, causing it to undergo Rabi oscillations.

Cross-resonance operation

- The most common application of cross-resonance is to implement a CNOT gate.
- Cross-resonance operations have been widely utilized in various experimental platforms for quantum computation, particularly in superconducting qubit architectures.
- The IBM superconducting transmon qubits have the cross-resonance operation with the effective Hamiltonian

$$H_{CR} = \frac{\sigma_z \otimes C}{2} + \frac{\mathbb{1}_2 \otimes D}{2},$$

with $C = \omega_{z\mathbf{1}}\mathbb{1}_2 + \omega_{zx}\sigma_x + \omega_{zy}\sigma_y + \omega_{zz}\sigma_z$ and $D = \omega_{\mathbf{1}x}\sigma_x + \omega_{\mathbf{1}y}\sigma_y + \omega_{\mathbf{1}z}\sigma_z$ [T. Alexander, et al., arXiv:2004.06755].

- The Hamiltonian term $\sigma_z \otimes \sigma_x$ is picked up and other unwanted terms are canceled by additional pulses. CNOT gate is local equivalent to $e^{i\pi\sigma_z\otimes\sigma_x/4}$.

Rescaled pulses for new two-qubit gates

- Finding the optimal parameters for the pulses is not an easy task. Classical machine learning may be helpful.

- To avoid the heavy calibrations, one can extract new gate from the calibrated pulses [P. Gokhale, et al., arXiv:2004.11205].

- The Gaussian square pulse has the area

$$\alpha = |A| \left(\omega + \sigma \sqrt{2\pi} \mathrm{erf}(n_\sigma) \right),$$

with the amplitude A, flat-top width ω, standard deviation σ of the Gaussian tails, and the truncated number n_σ.

- One can rescale the area according to $\alpha(\theta)/\alpha(\pi/2) = 2\theta/\pi$ in order to realize $e^{i\theta\sigma_z \otimes \sigma_x/2}$.

Braid gates

- Two-qubit gates $\check{B}$ satisfying

$$(\check{B} \otimes \mathbb{1})(\mathbb{1} \otimes \check{B})(\check{B} \otimes \mathbb{1}) = (\mathbb{1} \otimes \check{B})(\check{B} \otimes \mathbb{1})(\mathbb{1} \otimes \check{B}),$$

  are called the braid gates.

- All 4×4 solutions of braid matrices and braid gates are known [J. Hietarinta, arXiv:hep-th/9210067; H. A. Dye, arXiv:quant-ph/0211050].

- Most of the solutions can generate entanglement therefore universal [L. H. Kauffman, S. J. Lomonaco Jr., arXiv:quant-ph/0401090].

Braid gates

Consider the eight-vertex-type two-qubit gates, all solutions of braid gates are

$$\check{B}_I = \begin{pmatrix} e^{i\varphi_1} & 0 & 0 & 0 \\ 0 & 0 & e^{i\varphi_2} & 0 \\ 0 & e^{i\varphi_3} & 0 & 0 \\ 0 & 0 & 0 & e^{i\varphi_4} \end{pmatrix}, \qquad \check{B}_{II} = \begin{pmatrix} 0 & 0 & 0 & e^{i\varphi_2} \\ 0 & e^{i\varphi_1} & 0 & 0 \\ 0 & 0 & e^{i\varphi_1} & 0 \\ e^{i\varphi_3} & 0 & 0 & 0 \end{pmatrix}$$

$$\check{B}_{III} = \begin{pmatrix} \cos\varphi_1 & 0 & 0 & \sin\varphi_1 e^{i\varphi_2} \\ 0 & -i\sin\varphi_1 & -\cos\varphi_1 & 0 \\ 0 & -\cos\varphi_1 & -i\sin\varphi_1 & 0 \\ -\sin\varphi_1 e^{-i\varphi_2} & 0 & 0 & \cos\varphi_1 \end{pmatrix},$$

$$\check{B}_{IV} = \frac{1}{\sqrt{2}} \begin{pmatrix} 1 & 0 & 0 & e^{i\varphi_1} \\ 0 & 1 & 1 & 0 \\ 0 & -1 & 1 & 0 \\ -e^{-i\varphi_1} & 0 & 0 & 1 \end{pmatrix}$$

Geometric representation

- The braid gates have the nonlocal parameters

$$\check{B}_I = \left[\frac{\pi}{2}, \frac{\pi}{2}, \frac{\pi}{2} - \frac{1}{2}(\varphi_2 + \varphi_3 - \varphi_1 - \varphi_4)\right], \qquad \check{B}_{III} = \left[\frac{\pi}{2}, \frac{\pi}{2}, \frac{\pi}{2} - 2\varphi_1\right],$$

$$\check{B}_{II} = \left[\frac{\pi}{2}, \frac{\pi}{2}, \frac{\pi}{2} - \frac{1}{2}(2\varphi_1 - \varphi_2 - \varphi_3)\right], \qquad \check{B}_{IV} = \left[\frac{\pi}{2}, 0, 0\right].$$

- Braid gates $\check{B}_I$, $\check{B}_{II}$, and $\check{B}_{III}$ belong to the same group of two-qubit gates. $\check{B}_{IV}$ is equivalent to CNOT up to single-qubit gates.

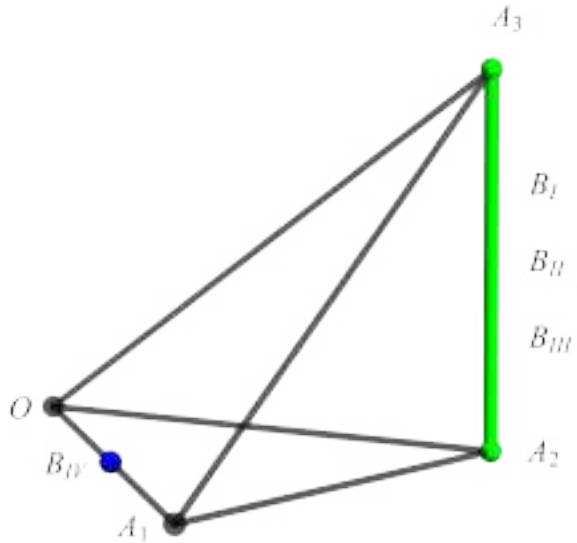

Decompositions of braid gates

Here we define $\phi_{I,1} = \frac{1}{2}(-\varphi_1 - \varphi_2 + \varphi_3 + \varphi_4)$, $\phi_{I,2} = \frac{1}{2}(-\varphi_1 + \varphi_2 - \varphi_3 + \varphi_4)$, $\phi_{I,3} = \frac{1}{2}(-\varphi_1 + \varphi_2 + \varphi_3 - \varphi_4)$, $\phi_{II,1} = \frac{1}{2}(-\varphi_2 + \varphi_3)$, and $\phi_{II,2} = \frac{1}{2}(-\varphi_2 + 2\varphi_1 - \varphi_3)$.

$B_I \cong$

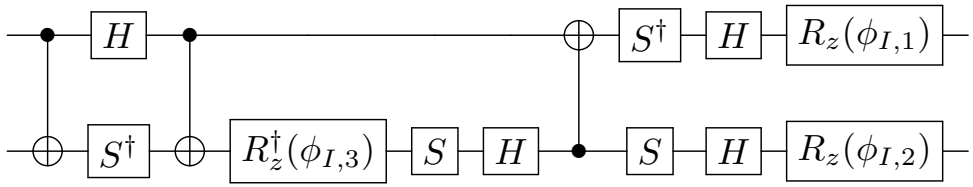

$B_{II} \cong$

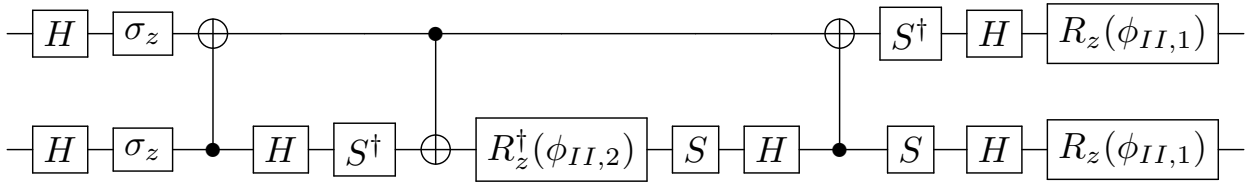

$B_{III} \cong$

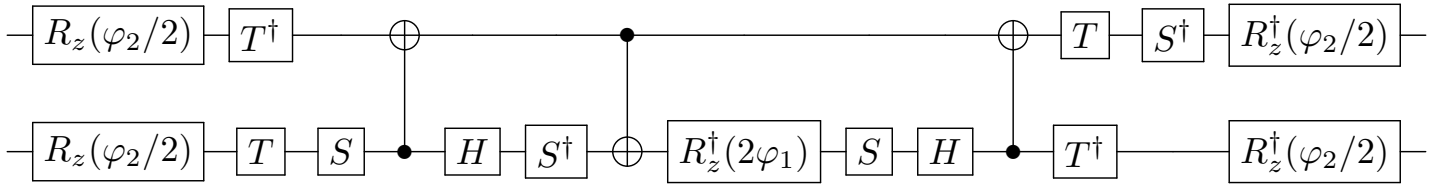

$B_{IV} \cong$

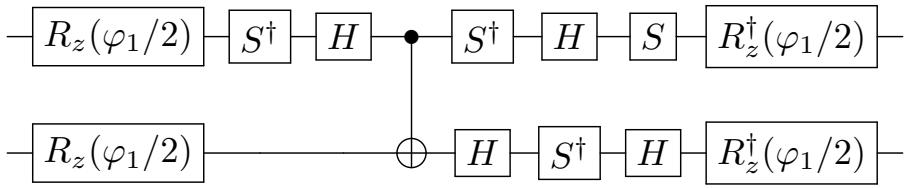

Yang-Baxterization

- Yang-Baxterization is a mathematical procedure to construct the solution of YBE from solution of braid relation proposed by [M. Jimbo, Lett. Math. Phys. 10, 63-69 (1985)]. Later it is generalized by [Y. Cheng, M. L. Ge, K. Xue, Comm. Math. Phys., 136, 195-208 (1991)].

- Suppose that the Braid operator has the spectral decomposition

$$\check{B} = \sum_{j=1}^{N} \lambda_j O_j,$$

with N distinct eigenvalues λ_j. The ansatz of $\check{R}$ matrix is given by

$$\check{R}(x) = \sum_{j=1}^{N} \rho_j(x) O_j,$$

$$\rho_1(x) = \left(x + \frac{\lambda_1}{\lambda_2}\right)\left(x + \frac{\lambda_2}{\lambda_3}\right)\cdots\left(x + \frac{\lambda_{N-1}}{\lambda_N}\right);$$
$$\rho_2(x) = \left(1 + x\frac{\lambda_1}{\lambda_2}\right)\left(x + \frac{\lambda_2}{\lambda_3}\right)\cdots\left(x + \frac{\lambda_{N-1}}{\lambda_N}\right);$$
$$\cdots$$
$$\rho_N(x) = \left(1 + x\frac{\lambda_1}{\lambda_2}\right)\left(1 + x\frac{\lambda_2}{\lambda_3}\right)\cdots\left(1 + x\frac{\lambda_{N-1}}{\lambda_N}\right).$$

Yang-Baxterization

- If the $\check{B}$ matrix has two distinct eigenvalues, such as $\check{B}_{IV}$, then we have

$$\check{R}(x) = \frac{1}{\lambda_2}\left(\check{B} + x\lambda_1\lambda_2\check{B}^{-1}\right).$$

- If the $\check{B}$ matrix has three distinct eigenvalues, such as $\check{B}_I(\varphi_1 = \varphi_4)$, $\check{B}_{II}$, and $\check{B}_{III}$, then we have

$$\check{R}(x) = \alpha(x)\check{B} + \beta(x)\mathbb{1} + \gamma(x)\check{B}^{-1},$$

The coefficients $\alpha(x)$, $\beta(x)$, and $\gamma(x)$ are given by

$$\alpha(x) = -\frac{1}{\lambda_3}(x-1), \qquad \beta(x) = \left(1 + \frac{\lambda_1}{\lambda_2} + \frac{\lambda_1}{\lambda_3} + \frac{\lambda_2}{\lambda_3}\right)x, \qquad \gamma(x) = \lambda_1 x(x-1).$$

It may not give the right R matrix. The permutations $(\lambda_1, \lambda_2, \lambda_3) \to (\lambda_2, \lambda_1, \lambda_3)$ and $(\lambda_1, \lambda_2, \lambda_3) \to (\lambda_1, \lambda_3, \lambda_2)$ may give different R matrices.

Yang-Baxter gates from $\check{B}_l$ including XXZ

- Define the parameters

$$\phi = \frac{1}{2}(\varphi_2 + \varphi_3) - \varphi_1, \qquad \alpha = \frac{1}{2}(\varphi_2 - \varphi_3), \qquad x = e^{\eta}.$$

- The braid gate $\check{B}_l$ with $\varphi_1 = \varphi_4$ gives the Yang-Baxter gates

$$\check{R}_{l,1}(\eta) \cong \begin{pmatrix} 1 & 0 & 0 & 0 \\ 0 & \dfrac{\sin\phi}{\sin(\phi - i\eta)} & \dfrac{-ie^{i\alpha}\sinh\eta}{\sin(\phi - i\eta)} & 0 \\ 0 & \dfrac{-ie^{-i\alpha}\sinh\eta}{\sin(\phi - i\eta)} & \dfrac{\sin\phi}{\sin(\phi - i\eta)} & 0 \\ 0 & 0 & 0 & 1 \end{pmatrix}.$$

$$\check{R}_{l,2}(\eta) \cong \begin{pmatrix} \sinh\left(\frac{1}{2}(\eta + i\phi)\right) & 0 & 0 & 0 \\ 0 & 0 & e^{i\alpha}\sinh\left(\frac{1}{2}(\eta - i\phi)\right) & 0 \\ 0 & e^{-i\alpha}\sinh\left(\frac{1}{2}(\eta - i\phi)\right) & 0 & 0 \\ 0 & 0 & 0 & \sinh\left(\frac{1}{2}(\eta + i\phi)\right), \end{pmatrix}$$

$$\check{R}_{l,3}(\eta) \cong \begin{pmatrix} \cosh\left(\frac{1}{2}(\eta + i\phi)\right) & 0 & 0 & 0 \\ 0 & 0 & e^{i\alpha}\cosh\left(\frac{1}{2}(\eta - i\phi)\right) & 0 \\ 0 & e^{-i\alpha}\cosh\left(\frac{1}{2}(\eta - i\phi)\right) & 0 & 0 \\ 0 & 0 & 0 & \cosh\left(\frac{1}{2}(\eta + i\phi)\right) \end{pmatrix}.$$

Yang-Baxter gates from $\check{B}_{II}$

- Define the parameters

$$\phi = \frac{1}{2}(\varphi_2 + \varphi_3) - \varphi_1, \qquad \alpha = \frac{1}{2}(\varphi_2 - \varphi_3), \qquad x = e^{\eta}.$$

- The braid gate $\check{B}_{II}$ gives the Yang-Baxter gates

$$\check{R}_{II,1}(\eta) \cong \begin{pmatrix} \dfrac{\sin\phi}{\sin(\phi - i\eta)} & 0 & 0 & \dfrac{-ie^{i\alpha}\sinh\eta}{\sin(\phi - i\eta)} \\ 0 & 1 & 0 & 0 \\ 0 & 0 & 1 & 0 \\ \dfrac{-ie^{-i\alpha}\sinh\eta}{\sin(\phi - i\eta)} & 0 & 0 & \dfrac{\sin\phi}{\sin(\phi - i\eta)} \end{pmatrix}$$

$$\check{R}_{II,2}(\eta) \cong \begin{pmatrix} 0 & 0 & 0 & e^{i\alpha}\sinh\left(\frac{1}{2}(\eta - i\phi)\right) \\ 0 & \sinh\left(\frac{1}{2}(\eta + i\phi)\right) & 0 & 0 \\ 0 & 0 & \sinh\left(\frac{1}{2}(\eta + i\phi)\right) & 0 \\ e^{-i\alpha}\sinh\left(\frac{1}{2}(\eta - i\phi)\right) & 0 & 0 & 0 \end{pmatrix}$$

$$\check{R}_{II,3}(\eta) \cong \begin{pmatrix} 0 & 0 & 0 & e^{i\alpha}\cosh\left(\frac{1}{2}(\eta - i\phi)\right) \\ 0 & \cosh\left(\frac{1}{2}(\eta + i\phi)\right) & 0 & 0 \\ 0 & 0 & \cosh\left(\frac{1}{2}(\eta + i\phi)\right) & 0 \\ e^{-i\alpha}\cosh\left(\frac{1}{2}(\eta - i\phi)\right) & 0 & 0 & 0 \end{pmatrix}$$

Yang-Baxter gates from $\check{B}_{III}$

The braid gate $\check{B}_{III}$ gives the Yang-Baxter gates

$$\check{R}_{III,1}(\eta) \cong \begin{pmatrix} \frac{\cosh\eta\cos\varphi_1}{\cosh(\eta+i\varphi_1)} & 0 & 0 & -e^{i\varphi_2}\frac{\sinh\eta\sin\varphi_1}{\cosh(\eta+i\varphi_1)} \\ 0 & i\frac{\cosh\eta\sin\varphi_1}{\sinh(\eta+i\varphi_1)} & -\frac{\sinh\eta\cos\varphi_1}{\sinh(\eta+i\varphi_1)} & 0 \\ 0 & -\frac{\sinh\eta\cos\varphi_1}{\sinh(\eta+i\varphi_1)} & i\frac{\cosh\eta\sin\varphi_1}{\sinh(\eta+i\varphi_1)} & 0 \\ e^{-i\varphi_2}\frac{\sinh\eta\sin\varphi_1}{\cosh(\eta+i\varphi_1)} & 0 & 0 & \frac{\cosh\eta\cos\varphi_1}{\cosh(\eta+i\varphi_1)} \end{pmatrix}$$

$$\check{R}_{III,2}(\eta) \cong \begin{pmatrix} \sinh\eta\cos\varphi_1 & 0 & 0 & e^{i\varphi_2}\cosh\eta\sin\varphi_1 \\ 0 & i\cosh\eta\sin\varphi_1 & -\sinh\eta\cos\varphi_1 & 0 \\ 0 & -\sinh\eta\cos\varphi_1 & i\cosh\eta\sin\varphi_1 & 0 \\ e^{-i\varphi_2}\cosh\eta\sin\varphi_1 & 0 & 0 & \sinh\eta\cos\varphi_1 \end{pmatrix}$$

$$\check{R}_{III,3}(\eta) \cong \begin{pmatrix} \cosh\eta\cos\varphi_1 & 0 & 0 & -e^{i\varphi_2}\sinh\eta\sin\varphi_1 \\ 0 & i\sinh\eta\sin\varphi_1 & -\cosh\eta\cos\varphi_1 & 0 \\ 0 & -\cosh\eta\cos\varphi_1 & i\sinh\eta\sin\varphi_1 & 0 \\ e^{-i\varphi_2}\sinh\eta\sin\varphi_1 & 0 & 0 & \cosh\eta\cos\varphi_1 \end{pmatrix}$$

Yang-Baxter gates from $\check{B}_{IV}$

- Define the parameter θ

$$\tan(\theta - \pi/4) = x.$$

- The braid gate $\check{B}_{IV}$ gives the uniqe Yang-Baxter gate

$$\check{R}_{IV}(\theta) = \begin{pmatrix} \cos\theta & 0 & 0 & e^{i\varphi_1}\sin\theta \\ 0 & \cos\theta & \sin\theta & 0 \\ 0 & -\sin\theta & \cos\theta & 0 \\ -e^{-i\varphi_1}\sin\theta & 0 & 0 & \cos\theta \end{pmatrix}.$$

Geometric representation

- The obtained Yang-Baxter gates $\check{R}_{I,1,2,3}$, $\check{R}_{II,1,2,3}$, $\check{R}_{III,1,2,3}$, and $\check{R}_{IV}$ can be categorized as three families.

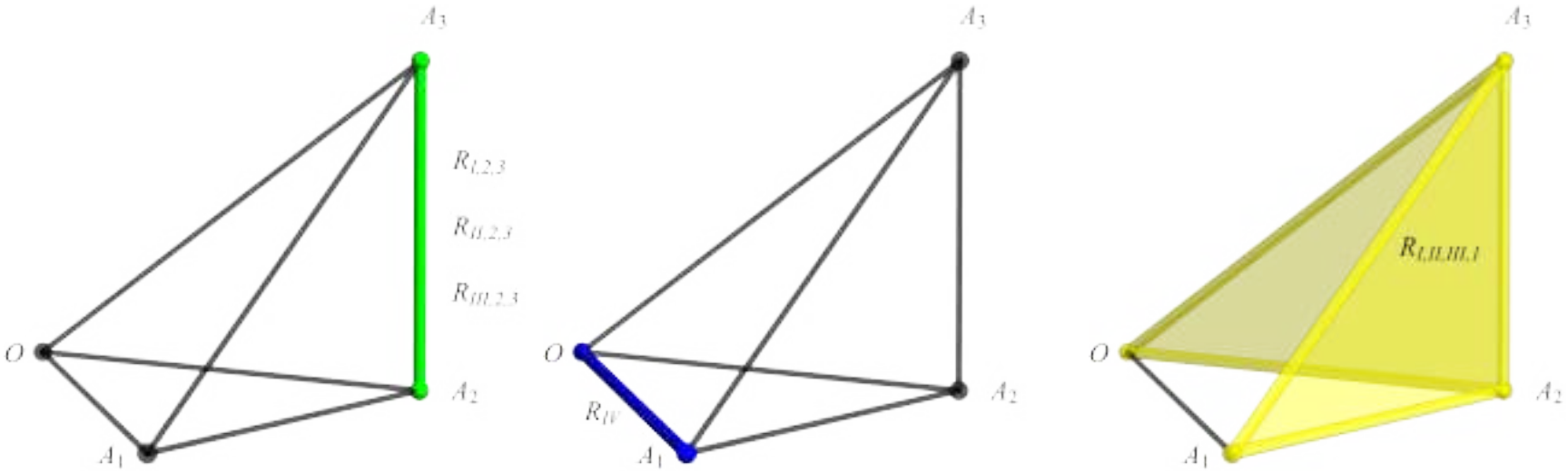

- Based on Theorem 1, the geometric representation can give the optimal gate decompositions.

Decompositions of Yang-Baxter gates

Here we define $\omega = \frac{1}{2}(\varphi_2 - \varphi_3)$. The parameters $a_{I,1}$, $c_{I,1}$, $\varphi_{I,2}$, and $\varphi_{I,3}$ are nonlocal parameters (tetrahedron parameters).

$R_{I,1} \cong$

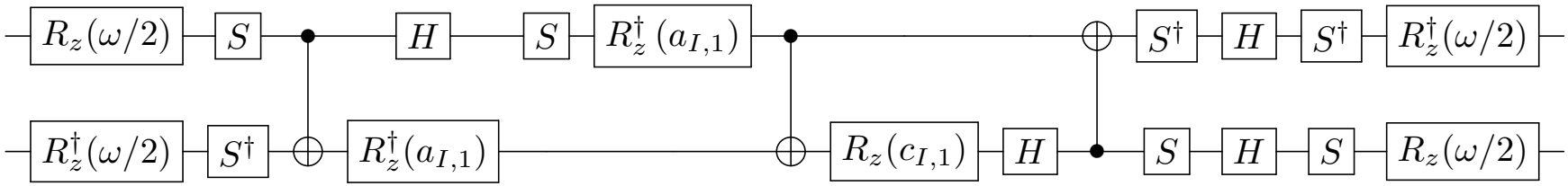

$R_{I,2} \cong$

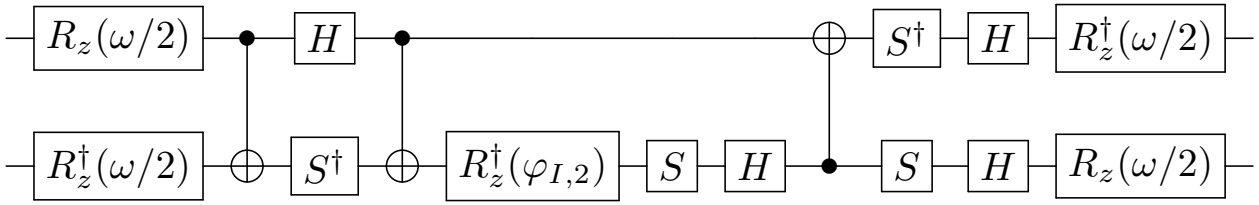

$R_{I,3} \cong$

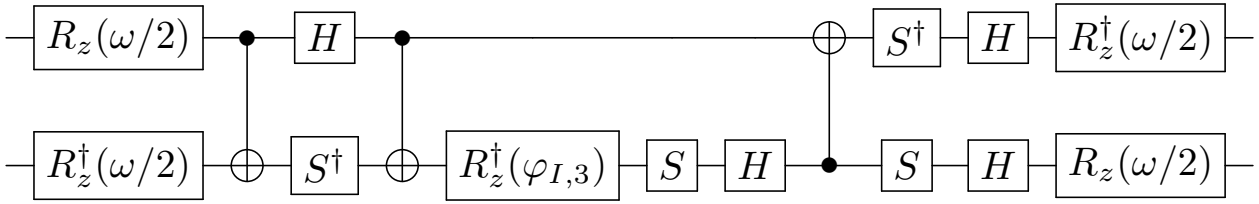

Decompositions of Yang-Baxter gates

Here the parameters $a_{III,1}$, $c_{III,1}$, $\varphi_{III,2}$, and $\varphi_{III,3}$ are nonlocal parameters (tetrahedron parameters).

$R_{III,1} \cong$

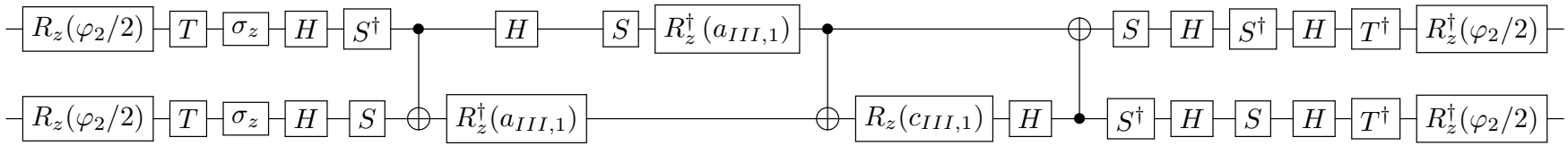

$R_{III,2} \cong$

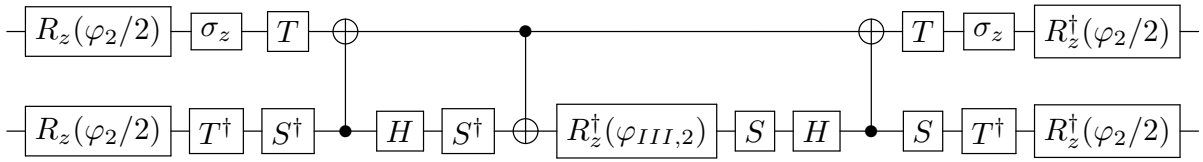

$R_{III,3} \cong$

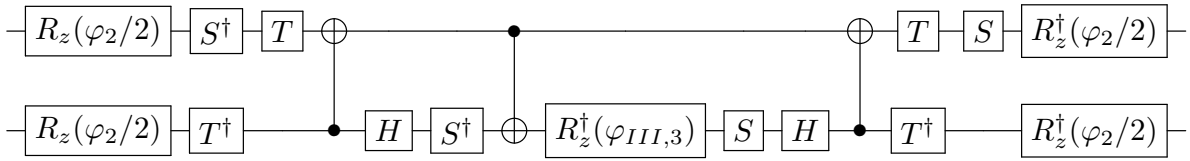

Entangling power

- The braid gate parameters φ_j and the spectral parameter η both determine the entangling power of the YBGs.

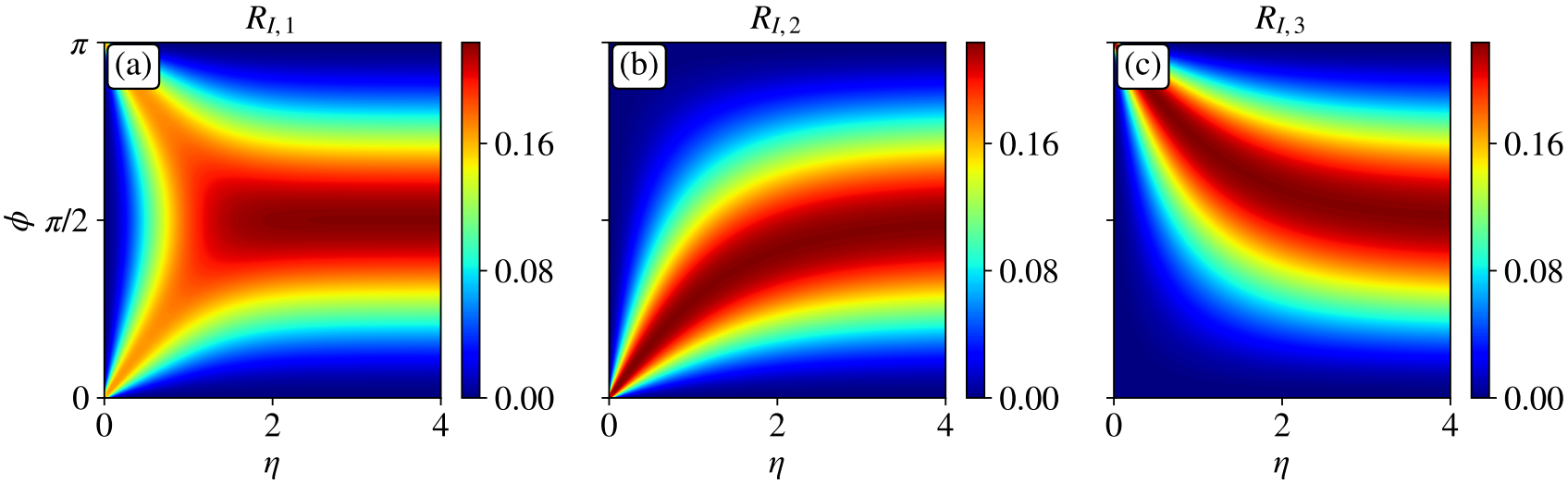

- The entangling power of $\check{R}_{II}$ and $\check{R}_{III}$ are similar with $\check{R}_{I}$.

Two examples

- Consider the YBG $\check{R}_{IV}$ obtained from the braid gate $\check{B}_{IV}$.

$$\check{R}_{IV}(\theta) = \begin{pmatrix} \cos\theta & 0 & 0 & e^{i\varphi_1}\sin\theta \\ 0 & \cos\theta & \sin\theta & 0 \\ 0 & -\sin\theta & \cos\theta & 0 \\ -e^{-i\varphi_1}\sin\theta & 0 & 0 & \cos\theta \end{pmatrix}.$$

- Consider the YBG $\check{R}_{XXX}(\phi)$ (belonging to $\check{R}_{I,1}$) from the Trotterization of XXX model with $\tan\phi = \mu$

$$\check{R}_{XXX}(\phi) = \frac{1+i\mu P}{1+i\mu} \cong \begin{pmatrix} e^{i\phi} & 0 & 0 & 0 \\ 0 & \cos\phi & i\sin\phi & 0 \\ 0 & i\sin\phi & \cos\phi & 0 \\ 0 & 0 & 0 & e^{i\phi} \end{pmatrix}.$$

Entangling properties of YBGs

- The entangling power of $\check{R}_{IV}(\theta)$ is

$$e_p\left(\check{R}_{IV}(\theta)\right) = \frac{2}{9}\sin^2(2\theta).$$

- The entangling power of $\check{R}_{XXX}(\phi)$ is

$$e_p\left(\check{R}_{XXX}(\phi)\right) = \frac{1}{6}\sin^2(2\phi).$$

- When $\theta = \pi/4$ or $\theta = 3\pi/4$, $\check{R}_{IV}(\theta)$ is the perfect entangler.

- When $\phi = \pi/4$ or $\phi = 3\pi/4$, $\check{R}_{XXX}(\phi)$ is the perfect entangler.

Gate realization of $\check{R}_{IV}(\theta)$

- The YBG $\check{R}_{IV}(\theta)$ requires minimal two CNOTs (superconducting quantum computers)

$\check{R}_{IV}(\theta) =$ 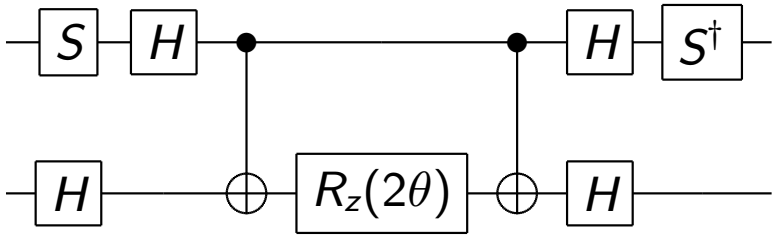

- The YBG $\check{R}_{IV}(\theta)$ requires minimal one R_{zz} (trapped-ion quantum computers)

$\check{R}_{IV}(\theta) =$ 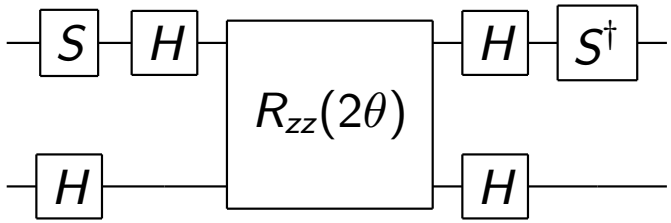

- When $\theta = \pi/4$, we have

$\check{R}_{IV}(\pi/4) =$ 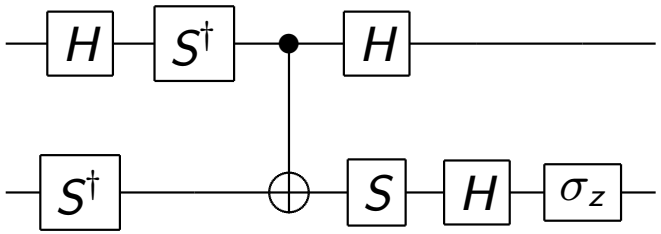

Pulse realization of $\check{R}_{IV}(\theta)$

Suppose that $\theta = \pi/3$. We have the pulses of (a) CNOT realization and (b) direct pulse construction.

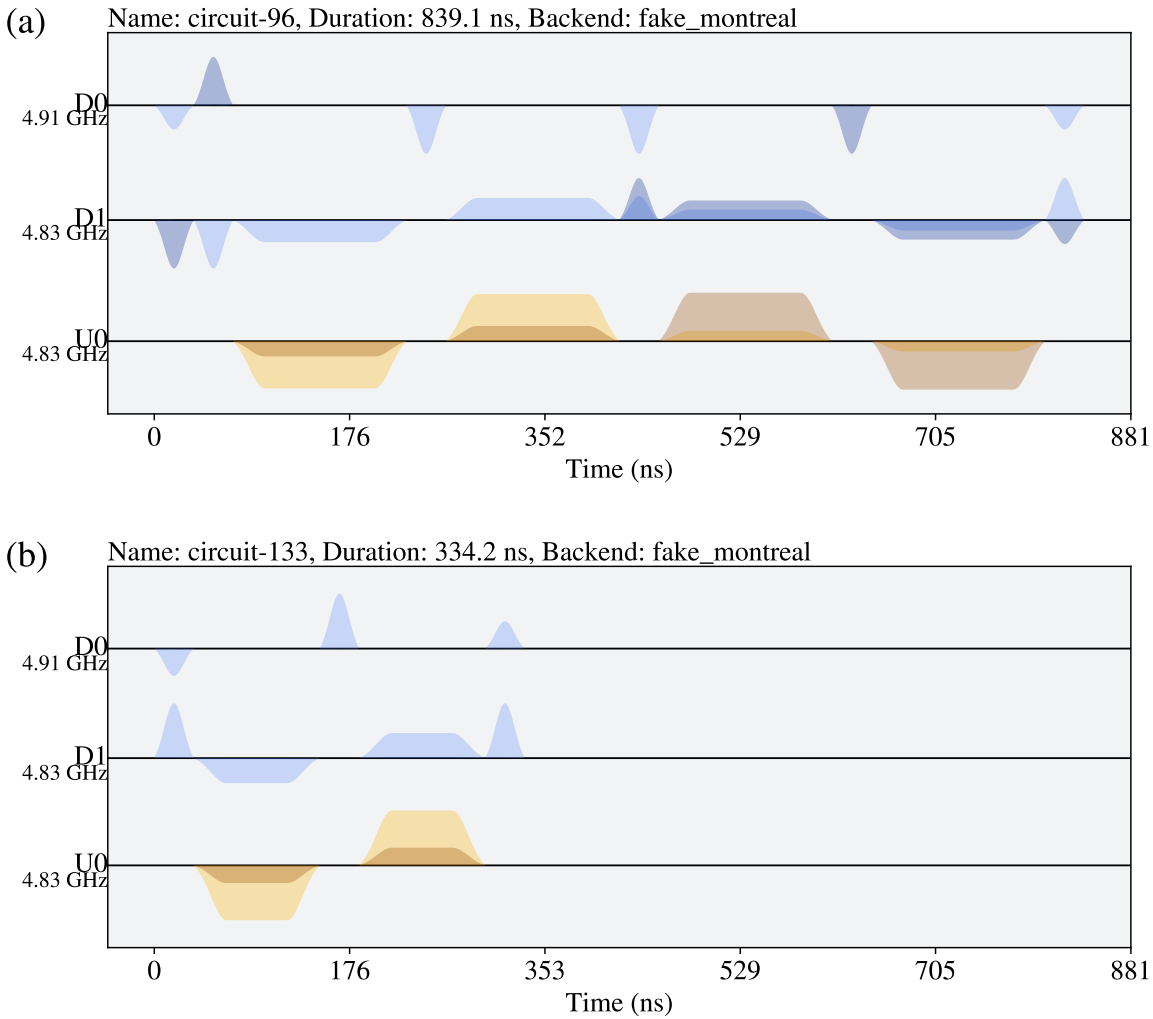

Gate fidelity of $\check{R}_{IV}(\theta)$

Gate fidelity from (a) simulator or (b) ibmq_montreal machine. (c) is the total pulse duration. (d) is the error reductions of pulse realization relative to other realizations.

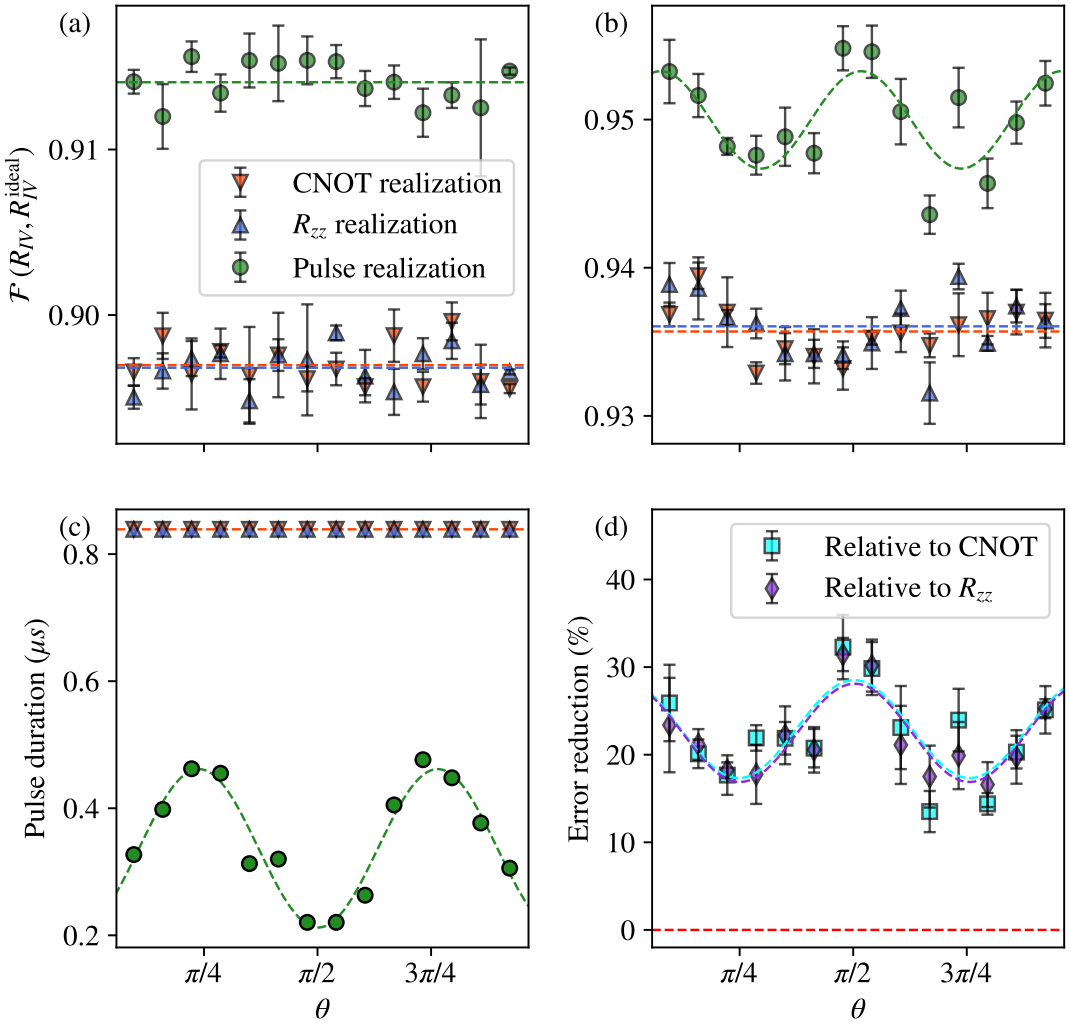

Gate realization of $\check{R}_{XXX}(\phi)$

- The YBG $\check{R}_{XXX}(\phi)$ requires minimal three R_{zz} (trapped-ion quantum computers)

$\check{R}_{XXX}(\phi) =$

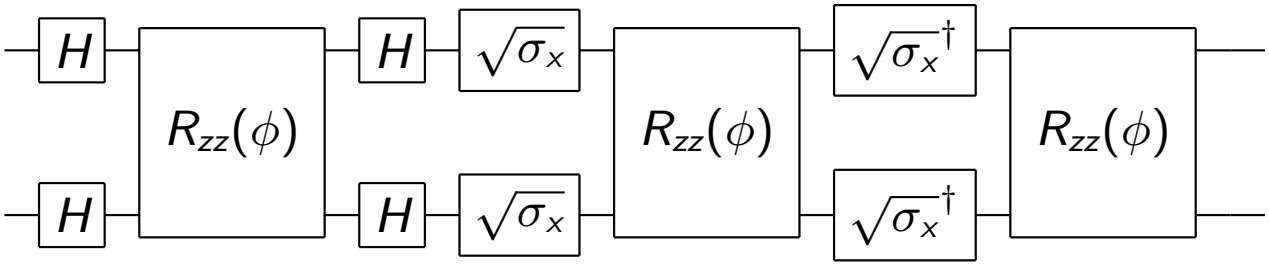

- The YBG $\check{R}_{XXX}(\phi)$ requires minimal three CNOTs (superconducting quantum computers)

$\check{R}_{XXX}(\phi) =$

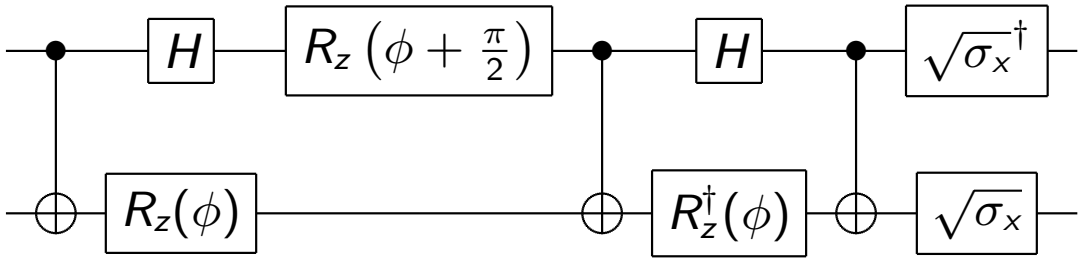

Pulse realization of $\check{R}_{xxx}(\phi)$

Suppose that $\phi = \pi/3$. We have the pulses of (a) CNOT realization, (b) R_{zz} realization, and (c) direct pulse construction.

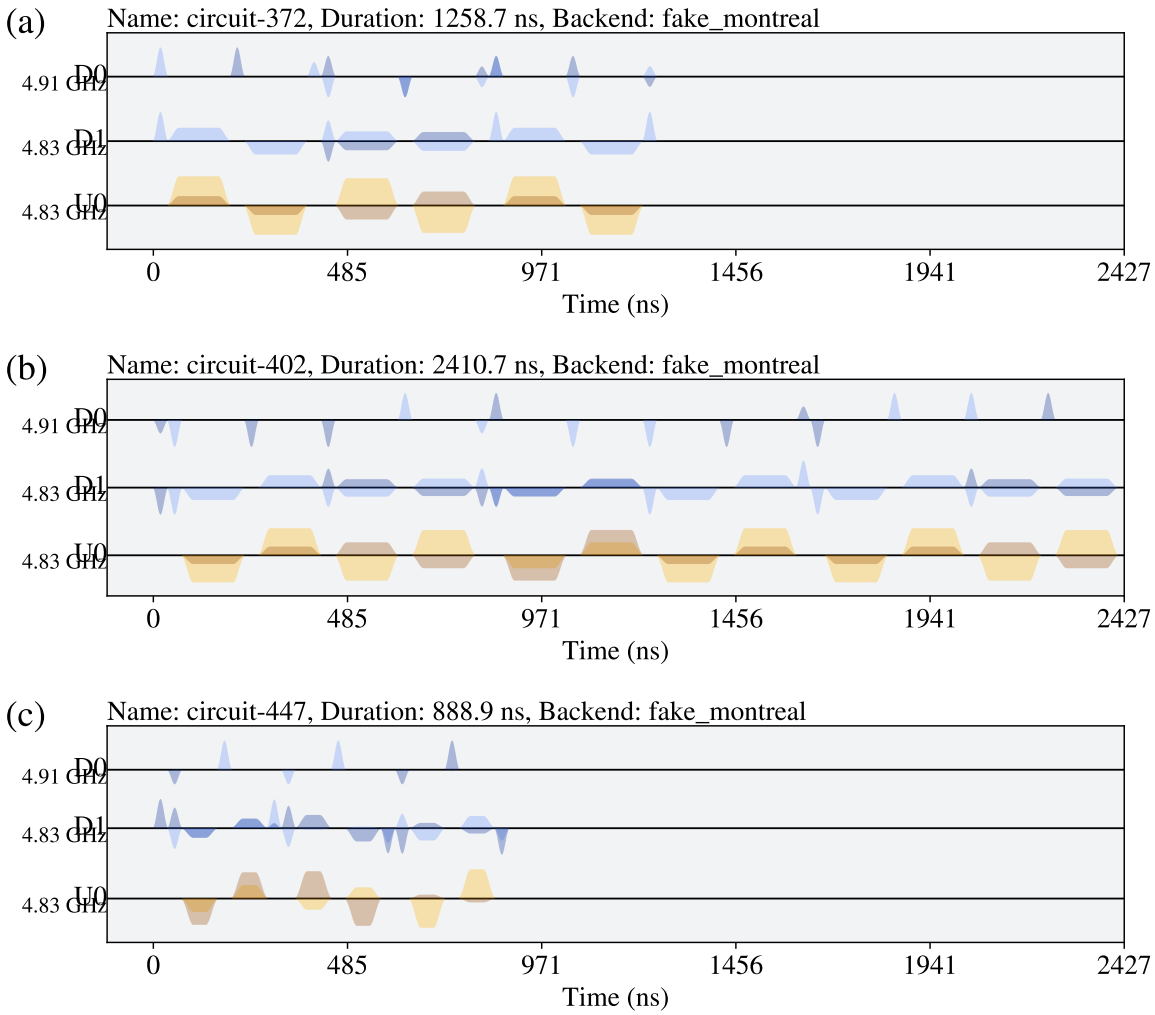

Gate fidelity of $\check{R}_{XXX}(\phi)$

Gate fidelity from (a) simulator or (b) ibmq_montreal machine. (c) is the total pulse duration. (d) is the error reductions of pulse realization relative to other realizations.

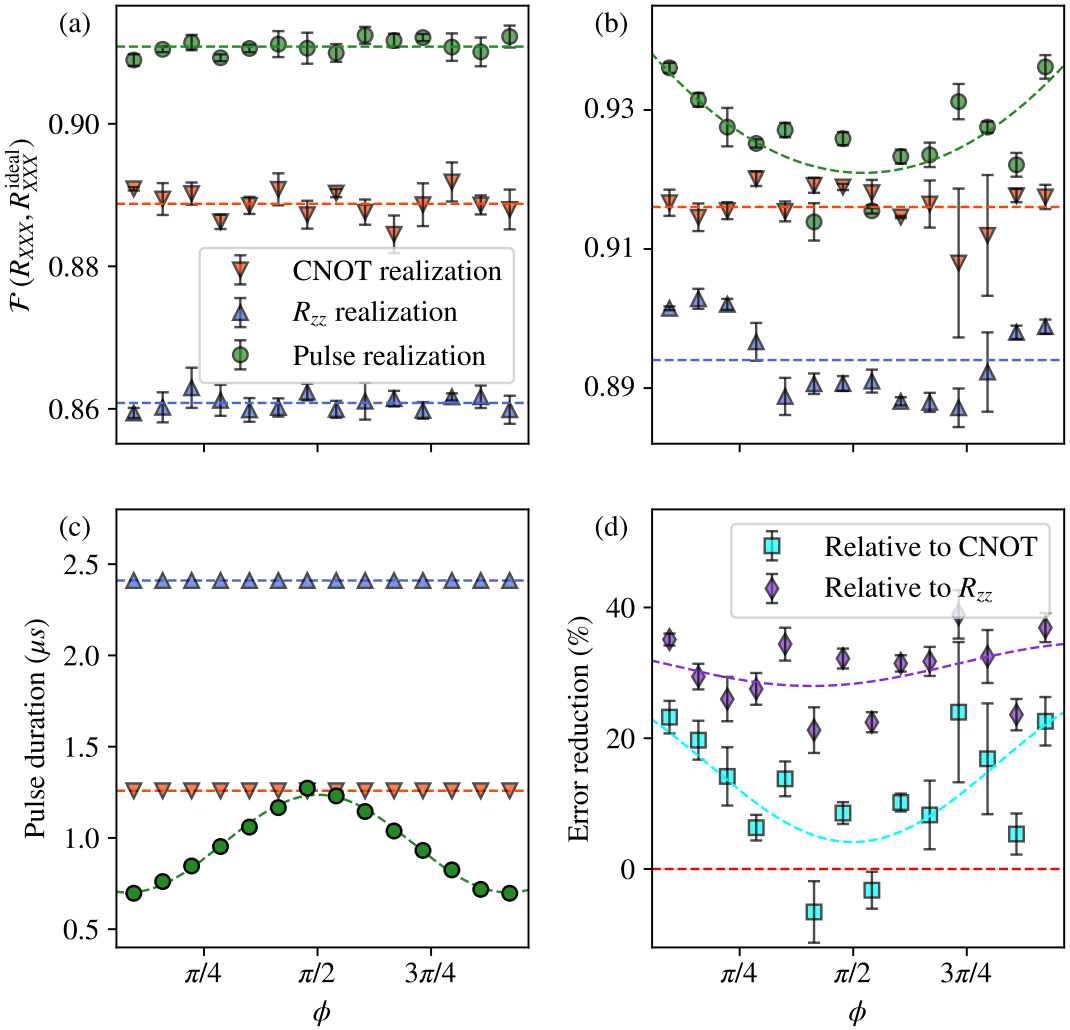

Conclusion

- The YBGs are the building blocks of the integrable circuits. It is a new method to study the far from equilibrium many-body quantum systems on quantum computers.
- The optimal constructions of YBGs can be obtained from their two-qubit geometric representations.
- YBGs realized from the pulse realization has the highest gate fidelities.
- In experiments, if two-qubit gates on the edge OA_1 and faces OA_2A_3 and $A_1A_2A_3$ can be constructed with high fidelity, then high-fidelity YBGs can be constructed (with some additional single-qubit gates).

Outlook

The quantum circuit model may be viewed as a generalized factorisable scattering model. It can also be viewed as a generalization of topological quantum computation [Y. Zhang, arXiv:1111.3940].

- TCIS: Trotter circuit of integrable system.
- IC: integrable circuit, which is composed of Yang-Baxter gates.
- LISC: logorithmic information spreading circuit, in which the information spreads logorithmic after a quench.
- QSC: quantum simulation circuit, which simulates the dynamics of physical system.
- Completely integrable many-qubit gates.

  Unitary solutions of the tetrahedron equations as gates

  `https://arxiv.org/pdf/2407.10731`

  will help us to compress circuits even more. The tetrahedron equations are higher dimensional version of Yang-Baxter equations.

Outlook